

## Removal of surfactant and capping agent from Pd nanocubes (Pd-NCs) using *tert*-butylamine: its effect on electrochemical characteristics

Cite this: *J. Mater. Chem. A*, 2013, **1**, 8553

N. Naresh,<sup>abc</sup> F. G. S. Wasim,<sup>abc</sup> B. P. Ladewig<sup>b</sup> and M. Neergat<sup>\*c</sup>

Synthesis of shape-controlled nanoparticles of precious metals with defined size is well-established in the literature and the control over shape and size is achieved using surfactants and capping agents. However, a clean surface without impurities is required for realistic applications. In the present investigation, palladium nanocubes are synthesized using poly(vinylpyrrolidone) and potassium bromide. A novel method for cleaning the nanoparticle surface, *i.e.*, treatment with *tert*-butylamine is reported. For comparison, a part of the untreated sample is subjected to the commonly used method of heat-treatment in an oxygen atmosphere for surface cleaning. The XPS and FTIR spectra of the heat-treated sample show incomplete removal of PVP and complete removal of Br<sup>-</sup> and the XRD pattern suggests oxide formation on the Pd surface. Treatment with *tert*-butylamine provides a clean surface free of PVP and Br<sup>-</sup>. Cleanliness of the surface is further confirmed by the voltammograms and ORR activities in 0.1 M HClO<sub>4</sub>. We conclude that *tert*-butylamine can be an effective solvent for the removal of PVP and a reagent for Br<sup>-</sup> ions because of its ability to form a quaternary ammonium salt.

Received 24th March 2013

Accepted 17th May 2013

DOI: 10.1039/c3ta11183k

[www.rsc.org/MaterialsA](http://www.rsc.org/MaterialsA)

### 1 Introduction

The physical and chemical properties of nanoparticles depend on their size, shape and composition. Size and shape control of nanoparticles is mostly achieved using surfactants and capping agents, and usually they are high molecular weight organic compounds with different functional groups. Some of the common surfactants are poly(vinylpyrrolidone) (PVP), sodium polyacrylate,<sup>1</sup> oleylamine,<sup>2</sup> and hexadecyl trimethyl ammonium bromide (CTAB).<sup>3,4</sup> Other than organic capping agents, inorganic salts such as KBr, KI, and KCN are also used for the synthesis of shape-controlled nanoparticles and the anions (I<sup>-</sup>, Br<sup>-</sup>, and CN<sup>-</sup>) strongly bind to the surface of the shape-controlled particles.<sup>5,6</sup> Thus, size and shape control has been reported with various materials for specific applications in different areas.

While strong adsorption characteristics of surfactants and capping agents on the initial nuclei of nanoparticles are important in controlling or arresting the crystal growth in selected directions, it is equally imperative to remove the adsorbed impurities from the nanoparticle surface after their synthesis. The strongly adsorbed impurities on the nanoparticle surface block the active sites and impacts negatively the

catalytic activity.<sup>7,8</sup> Thus, the ultrapure surface of shape-controlled nanoparticles, free of surfactants and capping agents, is critical for their application in catalysis.

The literature is replete with electrochemical characterization of catalysts for oxygen reduction reaction (ORR) on extended well-defined single crystal surfaces of Pt and to a certain extent with shape-controlled Pt nanoparticles.<sup>9-12</sup> At the same time, results on both single crystal surfaces and on shape-controlled nanoparticles of Pd are rarely reported in the literature, with only two recent reports known to the authors.<sup>13,14</sup> The major hurdle in obtaining reasonable electrochemical response and catalytic activity with shape-controlled Pd is getting a pure and clean surface.

Though selectivity above 80% of a particular shape is possible with nanoparticles in the size range of 3–10 nm, often, removal of the impurities (surfactant, capping, and stabilizing agents) from the surface of shape-controlled nanoparticles is challenging. Generally, in the literature, various methods are reported for the removal of adsorbed impurities from the nanoparticle surface. Each of the different surfactants and capping agents used has a unique interaction with the surface, and therefore, various cleaning methods are reported in the literature. Some of them are exposure to UV light, heat-treatment, acid/base washing, and alcohol washing.<sup>8,13,15</sup> The most established method has been the heat-treatment of stabilized nanoparticles in an oxidative atmosphere where the ligands are oxidized at 180–200 °C, followed by thorough washing of the heat-treated sample. At higher temperatures, there is a possibility of particle agglomeration and change in actual shape, and

<sup>a</sup>IITB-Monash Research Academy, Powai, Mumbai, India 400076

<sup>b</sup>Department of Chemical Engineering, Monash University, VIC 3800, Australia

<sup>c</sup>Department of Energy Science and Engineering, Indian Institute of Technology Bombay (IITB), Mumbai, India 400076. E-mail: [nmanoj@iitb.ac.in](mailto:nmanoj@iitb.ac.in); Fax: +91 22 2576 4890; Tel: +91 22 2576 7893

hence, proper control of temperature is required with the heat-treatment procedure.<sup>15</sup> In the acid/base treatment method, the prepared nanoparticles are treated in strong acidic/basic solutions for the removal of the surfactant, for example, removal of CTAB with NaOH solution. This treatment would be able to provide the replacement of strongly adsorbed organic impurities with soluble complexes that are easily washed away from the catalytic surfaces.<sup>13</sup> Another method of cleaning organic-ligands from the catalyst is by using UV-ozone exposure wherein the nanoparticles are treated in the UV-ozone atmosphere for the removal of PVP.<sup>8</sup> But, we cannot generalize the procedure for removal of impurities from the catalyst surface and it depends on the chemical nature of the surfactants and capping agents. Moreover, for catalytic applications, a proper method is yet to be established for the complete removal of organic impurities from the shape-controlled nanoparticles. Thus, the choice of the stabilizer removal is based on the chemical nature of organic-ligands and its adsorption strength with the catalyst surface. Some of the stabilizers interact strongly with the catalyst surface and some others do weakly.

In this manuscript, we report on the use of *tert*-butylamine (TBA) for the removal of KBr and PVP from Pd nanocubes (NCs). For comparison, the shape-controlled catalysts were also heat-treated in an oxygen atmosphere at  $\sim 200$  °C; this method was reported by Li *et al.* to remove the surfactant from Pt nanoparticles.<sup>7</sup> The same synthesis procedure with different reagents, conditions, and precursors may not result in the same kind of shape; similarly, the same cleaning procedure may not be suitable for removal of the surfactant from different shape-controlled materials.

## 2 Experimental details

### 2.1 Materials

Potassium tetrachloropalladate ( $K_2PdCl_4$ , 99.9% metal basis) from Alfa Aesar; L-ascorbic acid and poly(vinylpyrrolidone) (PVP,  $M_w$  40 000) from Sigma-Aldrich; potassium bromide (KBr), *tert*-butylamine (TBA) and all other solvents (acetone, hexane, isopropanol and ethanol) from Merck, India were used for the synthesis of the catalysts.

### 2.2 Synthesis of Pd nanocubes (Pd NCs)

The Pd NCs were synthesized by following the procedure reported in the literature.<sup>16</sup> In a round bottom flask, 8 mL of aqueous solution of PVP (105 mg), L-ascorbic acid (60 mg), and potassium bromide (KBr, 300 mg) were pre-heated in air at 80 °C for 15 min. Then, 3 mL of DI water containing  $K_2PdCl_4$  (57 mg) was added to the above solution. The reaction was allowed to proceed at 80 °C for 3 h. The product was collected by centrifugation and it was washed with acetone once and then 3–4 times with ethanol and *n*-hexane (1 : 3). Finally, the prepared Pd NCs were dispersed in 5 mL of ethanol solution.

### 2.3 Carbon-supported Pd nanocubes (Pd NCs)

The carbon-supported Pd NC catalyst of 20 wt% metal loading was prepared as follows: 80 mg of Vulcan XC-72 carbon was

added to 40 mL of ethanol and the mixture was sonicated for 30 min to get a uniform dispersion of carbon. To this carbon solution, 5 mL of ethanol containing 20 mg of Pd NCs was added and it was sonicated for 1 h and kept for overnight-stirring to ensure the homogeneity of metal nanoparticles on the carbon-support. Thereafter, the mixture was dried at 80 °C and it was thoroughly ground with a mortar and pestle.

### 2.4 Cleaning of as-prepared carbon-supported Pd NCs

The as-prepared carbon-supported Pd NCs were treated with TBA (catalyst : solvent 1(mg) : 2(mL)) for three days under stirring at room temperature. After the treatment, the catalyst was separated from the solvent by centrifugation at 6000 rpm for 10 min. The collected precipitate was washed with ethanol three times to remove excess surface-adsorbed amine. The final product was redispersed in ethanol and then dried over-night. For comparison of the effectiveness of the cleaning procedure, the as-prepared Pd NCs were subjected to heat-treatment at 200 °C for 3 h under an oxygen atmosphere. After heat-treatment, the catalyst was washed with ethanol.

## 3 Characterization

### 3.1 Physical characterization

The prepared samples were analyzed using a PANalytical X'Pert Pro machine (30 mA, 40 kV) with Cu  $K\alpha$  radiation of wavelength ( $\lambda$ ) 1.5406 Å with a step size of 0.07 from 10° to 90° at a scan rate of 0.6° per minute. The sample preparation procedure for transmission electron microscopy (TEM) is as follows: a small amount of the prepared catalyst was dispersed in ethanol and sonicated for 15 min to get a well-dispersed suspension of the nanoparticles and it was drop-cast on a copper grid. The prepared grid was dried under an IR lamp for a few minutes to remove any moisture content in the sample. The TEM images of the prepared samples were recorded using a JEOL JEM 2100 F field emission electron microscope operated at 200 kV. The Fourier-transform infrared spectra of the prepared samples were recorded using vertex 80 model, Bruker instruments. We used OPUS software for baseline correction, smoothing and peak assignment. The sample was prepared as follows: a small amount of the solid sample was mixed with KBr and it was made into a pellet-form by applying 5 Torr pressure using a compressor. The pellet was kept under the IR lamp for a few minutes to remove the moisture from the sample and it was loaded into the sample holder. The spectrum was collected by scanning the sample from 400 to 4000  $cm^{-1}$  with 4  $cm^{-1}$  spectral resolution and 32 scans. The XPS spectrum was recorded using a MultiLab Thermo VG Scientific spectrometer with Al  $K\alpha$  radiation of energy 1486.6 eV at a chamber pressure of *ca.*  $1.5 \times 10^{-7}$  Pa. For peak fitting, we used XPS Peak 4.1 software. The peaks were calibrated with the standard C1s peak fixed at 284.4 eV. Thermogravimetric analysis (TGA) of the samples was carried out using an SDT Q600, TA Instruments. The sample was heated up to 800 °C under a nitrogen atmosphere at a heating rate of 10 °C  $min^{-1}$ .

### 3.2 Electrochemical characterization

The electrochemical experiments were conducted by using a WaveDriver 20 Bipotentiostat/Galvanostat system from Pine Research Instrumentation, USA with a three-electrode electrochemical system. A double junction reference electrode (Ag/AgCl with saturated KCl), Pt wire counter electrode, and a glassy-carbon disk electrode were used for the electrochemical experiments. All potentials are reported against the reversible hydrogen electrode (RHE) in the manuscript. Catalyst ink was prepared by sonicating a mixture of 5 mg of catalyst with 5 mL of Millipore water, 10 mL of iso-propanol and 10  $\mu\text{L}$  of Nafion® solution (5 wt% solution from Sigma Aldrich) for 15 min. The well-dispersed ink was drop-cast on the glassy-carbon disk electrode (0.196  $\text{cm}^2$ ) to get a catalyst loading of 15  $\mu\text{g cm}^{-2}$ . The cyclic voltammogram (CV) was recorded using a rotating disc electrode (RDE) in an argon-saturated 0.1 M  $\text{HClO}_4$  solution at a scan rate of 20  $\text{mV s}^{-1}$ . After recording the CVs, a fresh electrolyte solution of 0.1 M  $\text{HClO}_4$  was saturated with oxygen and the ORR voltammogram was recorded at 1600 rpm with a scan rate of 20  $\text{mV s}^{-1}$ .

## 4 Results and discussion

The XRD patterns of the as-prepared, heat-treated, and TBA-cleaned Pd NCs are shown in Fig. 1. The patterns of the as-prepared and TBA-cleaned Pd NCs suggest that there is no change in the structure of the material after cleaning with TBA. The XRD pattern of the heat-treated catalyst exhibits some additional peaks when compared to that of the as-prepared and TBA-cleaned catalysts indicating the formation of oxides of Pd.

The TEM image of the as-prepared palladium NCs is shown in Fig. 2(a). The palladium NCs are well-dispersed on the carbon-support and the size of the palladium NCs is estimated to be  $\sim 6$  nm. The corresponding histogram and the high-resolution image are shown in the insets of Fig. 2(a). The high-resolution image confirms that the lattice spacing of the palladium NCs is 0.195 nm, the same as that of the standard (100) plane of Pd (JCPDS file no. 00-001-1201). The TEM images of the TBA-cleaned and heat-treated palladium NCs are presented in

Fig. 2(b) and (c). The image confirms that there is no change in the shape of the palladium NCs after cleaning with TBA and the size estimated is  $\sim 6$  nm. The corresponding histogram and high-resolution image are shown in the insets of Fig. 2(b). The morphological details of the as-prepared and TBA-cleaned palladium NCs suggest that our cleaning procedure for the removal of the stabilizer does not affect the shape and size of the particles.

To check the surface purity of the as-prepared, heat-treated, and TBA-cleaned catalysts, we analyzed the samples using XPS. Fig. 3 shows the C 1s XPS spectra of the as-prepared, heat-treated and TBA-cleaned Pd NCs along with that of Vulcan XC-72. The reduction in intensity of the XPS spectrum of the cleaned sample when compared to that of the as-prepared and heat-treated samples suggests that there is removal of the adsorbed surfactants from the catalyst surface with the TBA cleaning. Each spectrum can be deconvoluted into three peaks with different binding energies. The peak at 284.4 eV corresponds to graphitic carbon (C–C bonding). The binding energies of 285.9 and 287.8 eV correspond to the carbon in C–N and C=O, respectively.<sup>17</sup> The C–N and C=O groups belong to the pyrrolidone ring of the PVP, and from the XPS spectra, we can clearly see a significant reduction in the intensities of these peaks after treatment with TBA. The decrease in relative intensities of the peaks corresponding to C–N and C=O groups on TBA-treated Pd NCs suggests that PVP is removed from the surface but not in the case of the heat-treated sample. The peaks at 284.4 and 285.2 eV (shoulder peak), in the case of Vulcan XC-72, can be attributed to graphitic carbon and C–N. The additional peaks in the as-prepared and TBA-cleaned Pd NCs are from PVP interaction with the Pd nanoparticles. Thus, TBA-treatment is an efficient method to remove PVP from the surface of palladium NCs without changing the shape and size of the precious metal nanoparticles unlike the heat-treatment method.

Fig. 4 shows the XPS spectra of  $\text{Br}^-$  on the surface of the as-prepared, heat-treated, and TBA-cleaned Pd NCs. The  $\text{Br}^-$  spectrum of the as-prepared catalyst matches with the reported standard spectrum and it shows that the adsorbed  $\text{Br}^-$  exists on the surface.<sup>18</sup> The chemisorptive nature of  $\text{Br}^-$  ions makes their removal difficult during the initial washing; in such a case, heat-treatment is necessary.<sup>19</sup> The absence of a peak corresponding to  $\text{Br}^-$  in the case of heat-treated and TBA-treated samples clearly indicates that  $\text{Br}^-$  ions are removed from the surface. Our study suggests that TBA-cleaning can remove the  $\text{Br}^-$  ions and PVP from the catalyst surface without heat-treatment; the PVP and  $\text{Br}^-$  removal mechanism is discussed in the later section. To further confirm the removal of PVP from the TBA-cleaned Pd NCs, we carried out TGA of the samples. Fig. 5 shows TGA of the as-prepared and TBA-cleaned Pd NCs along with that of carbon (Vulcan XC-72) for comparison. We can observe a weight loss at temperatures below 250  $^\circ\text{C}$  in the as-prepared Pd NCs and carbon corresponding to the removal of adsorbed moisture and low-molecular weight oligomers. The as-prepared catalyst shows a significant weight loss above 250  $^\circ\text{C}$ , where the PVP starts decomposing. At 450  $^\circ\text{C}$ , the weight loss with the TBA-cleaned sample is  $\sim 9\%$ , whereas that with the as-prepared

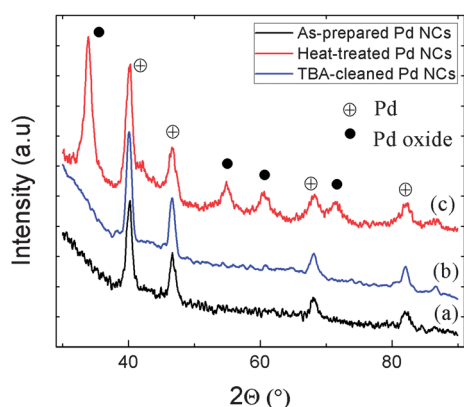


**Fig. 1** XRD patterns of the carbon-supported Pd NCs: (a) as-prepared, (b) TBA-treated, and (c) heat-treated.

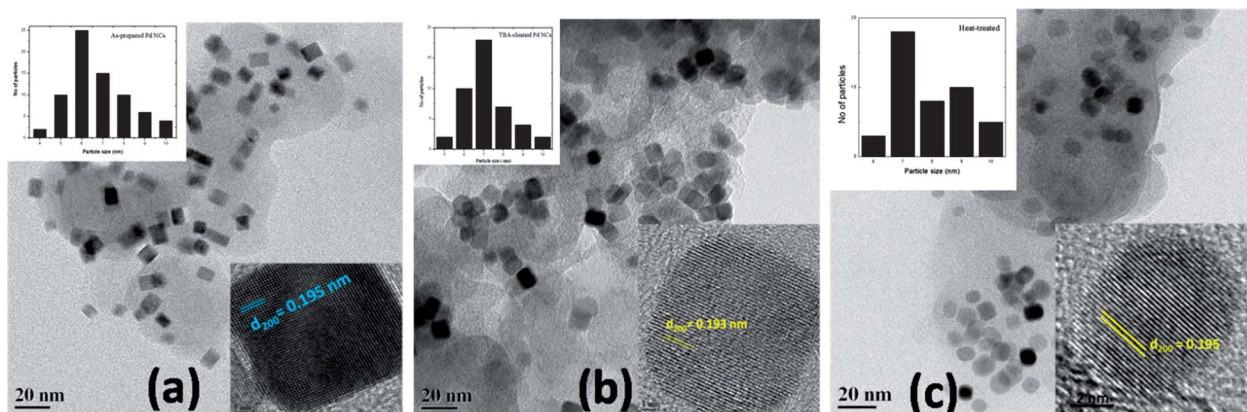


**Fig. 2** TEM images of carbon-supported Pd NCs: (a) as-prepared, (b) TBA-treated, and (c) heat-treated. The insets show the corresponding particle size distribution and high resolution images.

catalyst is 20%. The complete decomposition of PVP takes place in the temperature range of 250–650 °C.<sup>20,21</sup> However, a slight and gradual decrease in weight can also be seen for the TBA-cleaned sample above 300 °C; this may be attributed to the traces of PVP left in the sample. The sudden weight loss beyond ~650 °C is due to the oxidation of carbon which can be observed clearly from all the samples.<sup>22</sup> Moreover, the presence of Pd in our catalysts may catalyze the oxidation of carbon and contribute to the weight-loss at low temperatures because of the trace amount of oxygen impurity (in the form of adsorbed-oxygen on both carbon and Pd). Along with XPS, FTIR and electrochemical data, the TGA analysis also confirms the effectiveness of our cleaning procedure.

The infrared spectra of the as-prepared and TBA-treated palladium NCs are shown in Fig. 6. For reference, the spectrum of pure PVP is also shown in Fig. 6 and the frequency of the characteristic vibrational modes of PVP matches very well with

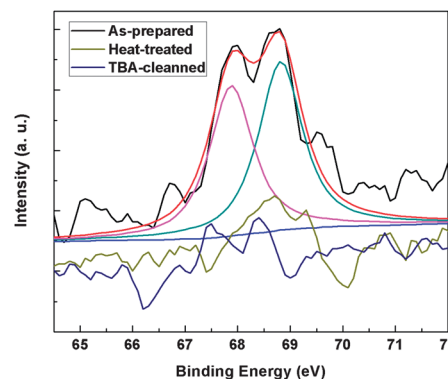


**Fig. 4** XPS spectra of Br<sup>-</sup> ions in carbon-supported as-prepared, heat-treated, and TBA-cleaned catalysts.

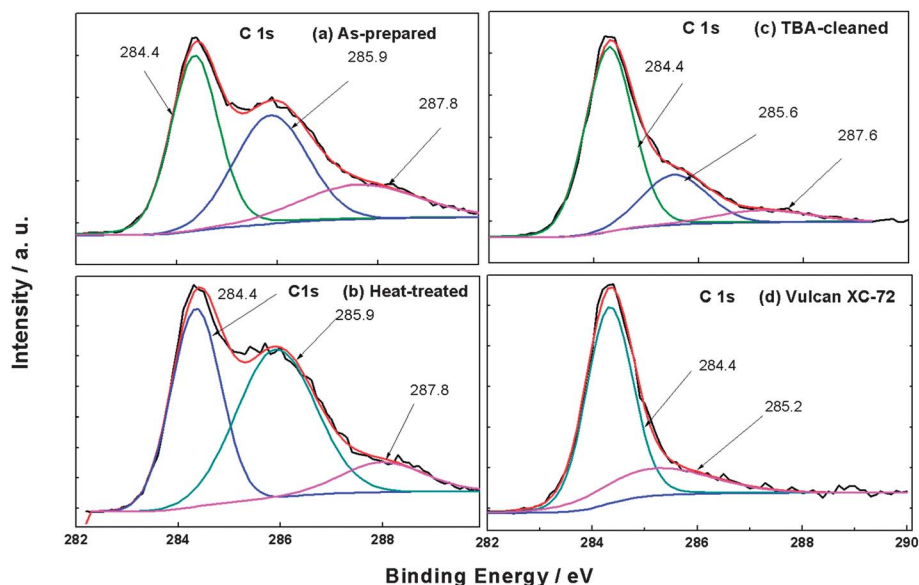


**Fig. 3** High resolution C 1s XPS spectra of carbon-supported Pd NCs: (a) as-prepared, (b) heat-treated, (c) TBA-cleaned and (d) Vulcan XC-72.



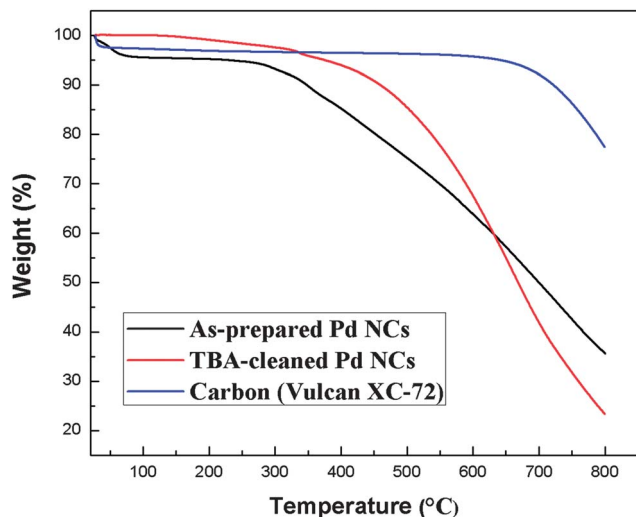


**Fig. 5** Thermogravimetric analysis of carbon-supported Pd NCs: (a) as-prepared, (b) TBA-cleaned, and (c) Vulcan XC-72.

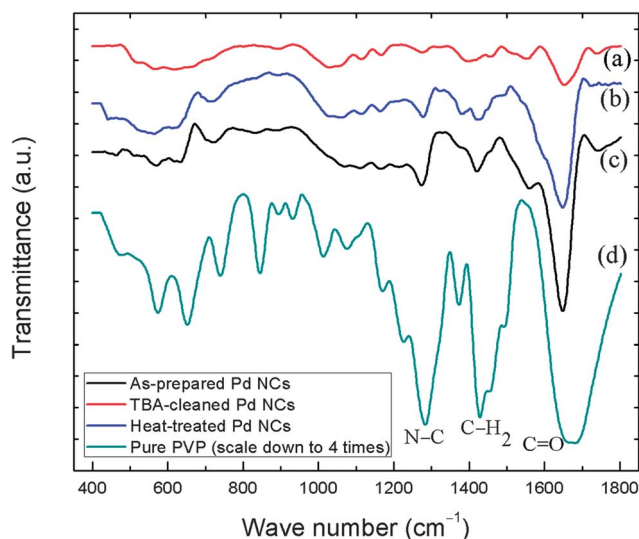


**Fig. 6** FTIR spectra of carbon-supported Pd NCs: (a) TBA-treated, (b) heat-treated, (c) as-prepared samples, and (d) pure PVP from 400  $\text{cm}^{-1}$  to 1800  $\text{cm}^{-1}$ .

that reported in the literature.<sup>23,24</sup> Transmittance of characteristic peaks of PVP (C=O; C-H<sub>2</sub>; C-H; C-N) on Pd NCs is in the following order: as-prepared > heat-treated > TBA-cleaned and this suggests that the excess PVP could be removed from the catalyst surface and treatment with TBA results in almost complete removal of PVP.

The effectiveness of different cleaning procedures in revealing the true electrocatalytic activity of the NCs is examined using electrochemical methods. The cyclic voltammograms of the as-prepared, heat-treated and TBA-treated catalysts are shown in Fig. 7. The precious metal loading on the glassy-carbon disk is 15  $\mu\text{g cm}^{-2}$ . Generally, the CV of precious metals like Pd shows features such as  $H_{\text{upd}}$  from 0.04 to 0.4 V followed by a double layer region from 0.4 to 0.7 V, and finally an oxide formation region above 0.7 V.<sup>25</sup> From the figure, we

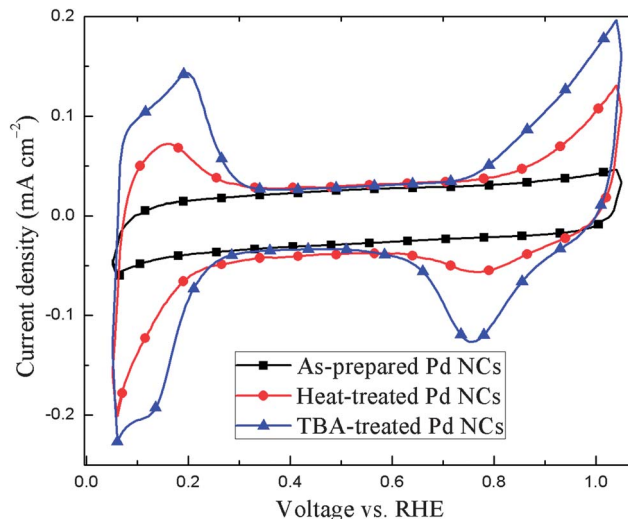


**Fig. 7** Cyclic voltammograms of the carbon-supported as-prepared, heat-treated, and TBA-treated catalysts in argon-saturated 0.1 M  $\text{HClO}_4$  solution at 20  $\text{mV s}^{-1}$  scan rate.

can clearly observe that an as-prepared catalyst does not show any of the characteristic features of palladium on potential cycling. This is because the surface of palladium is completely covered with capping agent and stabilizers like  $\text{Br}^-$  and PVP; it blocks the catalyst surface from electrolyte and the faradic reactions will not take place, only the non-faradic double layer charging can be observed.  $\text{Br}^-$  ions adsorb very strongly onto the palladium surface and their removal is a very difficult task. Similarly, the PVP molecule will get adsorbed on the Pd surface and the oxygen and nitrogen atoms from the pyrrolidone ring of PVP will interact with the Pd surface.<sup>23</sup> The long organic chain of PVP hinders the diffusion of reactants towards the surface of palladium. Heat-treatment of the catalyst partially removes some amount of capping agent and stabilizer from the surface of Pd; this is evident from the CVs. Clear features of palladium can be observed for samples treated with TBA and the overall voltammetric features suggest that it effectively removes both  $\text{Br}^-$  and PVP. There is a sharp peak at  $\sim 0.2$  V in the  $H_{\text{upd}}$  region due to the hydrogen desorption from {100} planes since the cubic structure is dominant with {100} planes.<sup>13</sup> The oxide formation is also high and there is a very large oxide reduction peak at  $\sim 0.75$  V in the reverse scan. Fig. 8 shows ORR voltammograms of all the catalysts recorded in oxygen-saturated 0.1 M  $\text{HClO}_4$  solution. The as-prepared Pd nanocubes do not show any appreciable current due to ORR. After heat-treatment of the catalyst, the ORR voltammogram shows an onset of current due to ORR at fuel cell-relevant operating potential (0.8 V) with a limiting current of 4  $\text{mA cm}^{-2}$ . The TBA-treated catalyst shows significant current due to ORR when compared to that of the as-prepared and heat-treated samples, and it matches with that of the standard Pd reported in the literature.<sup>26</sup> Three distinct regions can be clearly observed; there is a well-defined mass-transfer limited current region below 0.7 V and the current above 0.7 V is due to the ohmic and activation-limited region.

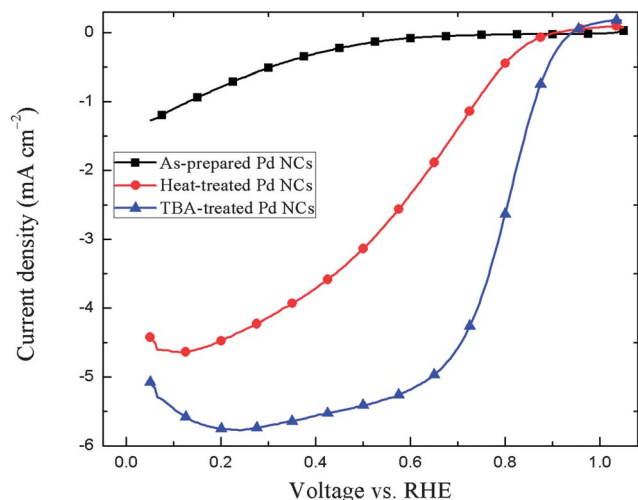


**Fig. 8** Oxygen reduction reaction voltammograms of carbon-supported as-prepared, heat-treated, and TBA-treated catalysts in oxygen-saturated 0.1 M HClO<sub>4</sub> solution at 20 mV s<sup>-1</sup> scan rate with 1600 rpm.

#### 4.1 Proposed mechanism of surfactant and capping agent removal from the catalyst surface

For the synthesis of Pd NCs, PVP has been used for stabilizing the nanoparticles whereas Br<sup>-</sup> ions are helpful in controlling the growth in selected directions (in this case (100)). After synthesis, Pd nanoparticles are separated from the solution by removing the excess PVP and Br<sup>-</sup> ions, but traces of the adsorbed species still remain on the catalyst surface which is confirmed from both the physical and electrochemical characterizations. The carbon-supported Pd NCs are dispersed in TBA and the mixture is kept under stirring for three days at room

temperature. With the dissolving nature of PVP in organic solvents (*e.g.*, polar compounds dissolve in polar solvents), most of the remaining PVP can be removed with the prolonged treatment in TBA. Simultaneously, Br<sup>-</sup> ions at the surface of the NCs could be removed due to the salt formation capability of amines with Br<sup>-</sup> ions. The complete removal of the Br<sup>-</sup> ions is also confirmed by the XPS spectra and the clean CV features. With the heat-treatment, only the removal of chemisorbed Br<sup>-</sup> ions from the catalyst surface is possible, and not that of PVP; this is confirmed by XPS analysis shown in Fig. 4. The relatively strong interaction between PVP and Pd may be the reason for its incomplete removal. The schematic representation of the extent of cleaning achieved with TBA and heat-treatment is shown in Fig. 9.

## 5 Conclusions

Removal of surfactant and capping agent on palladium NCs is carried out at room temperature using *tert*-butylamine and heat-treatment at 200 °C. Among these procedures, *tert*-butylamine treatment is found to be the best method for the removal of adsorbed-surfactant and capping agent from the catalyst surface. HRTEM images and the XRD patterns indicate that treatment with TBA does not distort the shape of the particle. The very low intensity of peaks corresponding to Br<sup>-</sup> and C=O groups in the FTIR and XPS spectra suggests that *tert*-butylamine is an efficient solvent to remove surfactant and capping agent from the shape-controlled catalyst surface. At the same time, heat-treatment results in Pd oxide formation and partial removal of the impurities from the Pd surface. The treated catalysts are subjected to electrochemical characterization under acidic conditions. The voltammetric features and

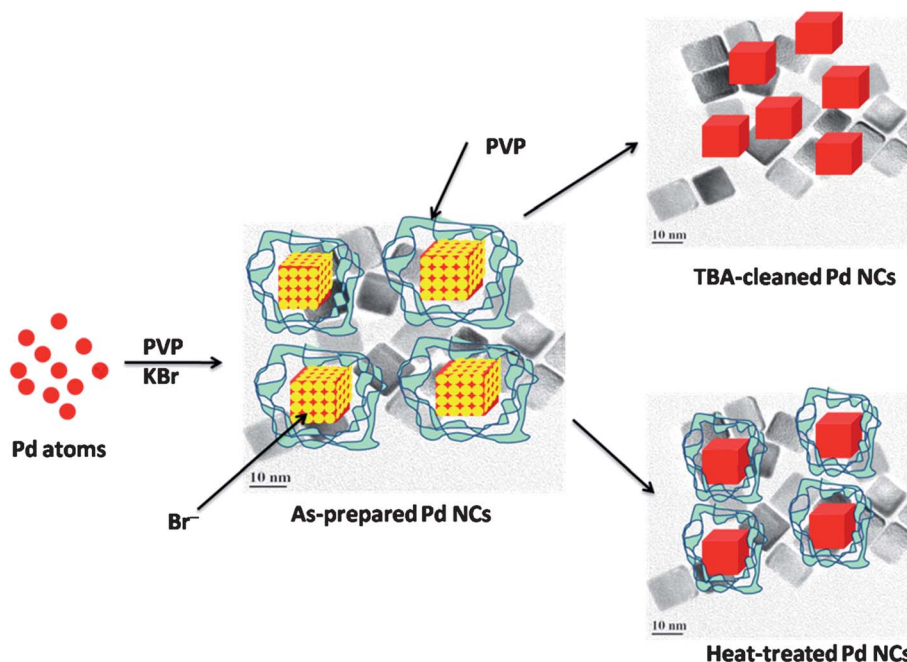


**Fig. 9** Scheme proposed for the removal of the stabilizer and capping agent from the catalyst surface.

ORR activities of the TBA-treated catalysts in 0.1 M HClO<sub>4</sub> further confirm effective removal of the surfactant and capping agent. We conclude that *tert*-butylamine can be an effective solvent for the removal of PVP and a reagent for Br<sup>-</sup> ions because of its ability to form a quaternary ammonium salt.

## Acknowledgements

The authors would like to sincerely thank the Department of Science and Technology (DST), Government of India, for funding the project (Grant No. SR/S1/PC-68/2012). The authors would also like to thank Sophisticated Analytical Instrument Facility (SAIF) for HR-TEM, and FTIR facilities, Department of Metallurgical Engineering and Material Science for XRD and TGA, and Department of Physics for XPS; all the facilities are at IIT Bombay.

## References

- 1 T. S. Ahmadi, Z. L. Wang, T. C. Green, A. Henglein and M. A. El-Sayed, *Science*, 1996, **272**, 1924.
- 2 J. Ren and R. D. Tilley, *Small*, 2007, **3**, 1508.
- 3 Y. Sun, L. Zhang, H. Zhou, Y. Zhu, E. Sutter, Y. Ji, M. H. Rafailovich and J. C. Sokolov, *Chem. Mater.*, 2007, **19**, 2065.
- 4 B. Veisz and Z. Kiraly, *Langmuir*, 2003, **19**, 4817.
- 5 Y. Xia, Y. Xiong, B. Lim and S. E. Skrabalak, *Angew. Chem., Int. Ed.*, 2009, **48**, 60.
- 6 T. H. Ha, H.-J. Koo and B. H. Chung, *J. Phys. Chem. C*, 2007, **111**, 1123.
- 7 D. Li, C. Wang, D. Tripkovic, S. Sun, N. M. Markovic and V. R. Stamenkovic, *ACS Catal.*, 2012, **2**, 1358.
- 8 M. Crespo-Quesada, J.-M. Andanson, A. Yarulin, B. Lim, Y. Xia and L. Kiwi-Minsker, *Langmuir*, 2011, **27**, 7909.
- 9 N. M. Markovic, H. A. Gasteiger and P. N. Ross, *J. Phys. Chem.*, 1996, **100**, 6715.
- 10 N. M. Markovic, R. R. Adzic, B. D. Cahan and E. B. Yeager, *J. Electroanal. Chem.*, 1994, **377**, 249.
- 11 F. J. Vidal-Iglesias, R. M. Aran-Ais, J. Solla-Gullón, E. Herrero and J. M. Feliu, *ACS Catal.*, 2012, **2**, 901.
- 12 J. Solla-Gullón, P. Rodriguez, E. Herrero, A. Aldaz and J. M. Feliu, *Phys. Chem. Chem. Phys.*, 2008, **10**, 1359.
- 13 H. Erikson, A. Sarapuu, N. Alexeyeva, K. Tammeveski, J. Solla-Gullón and J. M. Feliu, *Electrochim. Acta*, 2012, **59**, 329.
- 14 C.-L. Lee and H.-P. Chiou, *Appl. Catal., B*, 2012, **117–118**, 204.
- 15 Z. L. Wang, J. M. Petroski, T. C. Green and M. A. El-Sayed, *J. Phys. Chem. B*, 1998, **102**, 6145.
- 16 M. Jin, H. Liu, H. Zhang, Z. Xie, J. Liu and Y. Xia, *Nano. Res.*, 2011, **4**, 83–91.
- 17 C. Shan, H. Yang, J. Song, D. Han, A. Ivaska and L. Niu, *Anal. Chem.*, 2009, **81**, 2378.
- 18 K. Shimizu, A. Shchukarev, P. A. Kozin and J.-F. Boily, *Langmuir*, 2013, **29**, 2623.
- 19 H.-C. Peng, S. Xie, J. Park, X. Xia and Y. Xia, *J. Am. Chem. Soc.*, 2013, **135**, 3780.
- 20 C. Peniche, D. Zaldivar, M. Pazos, S. Paz, A. Bulay and J. S. Roman, *J. Appl. Polym. Sci.*, 1993, **50**, 485.
- 21 C. Kim and H. Lee, *Catal. Commun.*, 2009, **10**, 1305.
- 22 Y. L. Hsin, K. C. Hwang and C.-T. Yeh, *J. Am. Chem. Soc.*, 2007, **129**, 9999.
- 23 J. Xian, Q. Hua, Z. Jiang, Y. Ma and W. Huang, *Langmuir*, 2012, **28**, 6736.
- 24 J. Bai, Y. Li, C. Zhang, X. Liang and Q. Yang, *Colloids Surf., A*, 2008, **329**, 165.
- 25 M. Neergat and R. Rahul, *J. Electrochem. Soc.*, 2012, **159**, F234.
- 26 M. Neergat, V. Gunasekar and R. Rahul, *J. Electroanal. Chem.*, 2011, **658**, 25.